NATIONAL HURRICANE RESEARCH PROJECT

REPORT NO. 53

On the Momentum and Energy Balance of Hurricane Helene (1958)

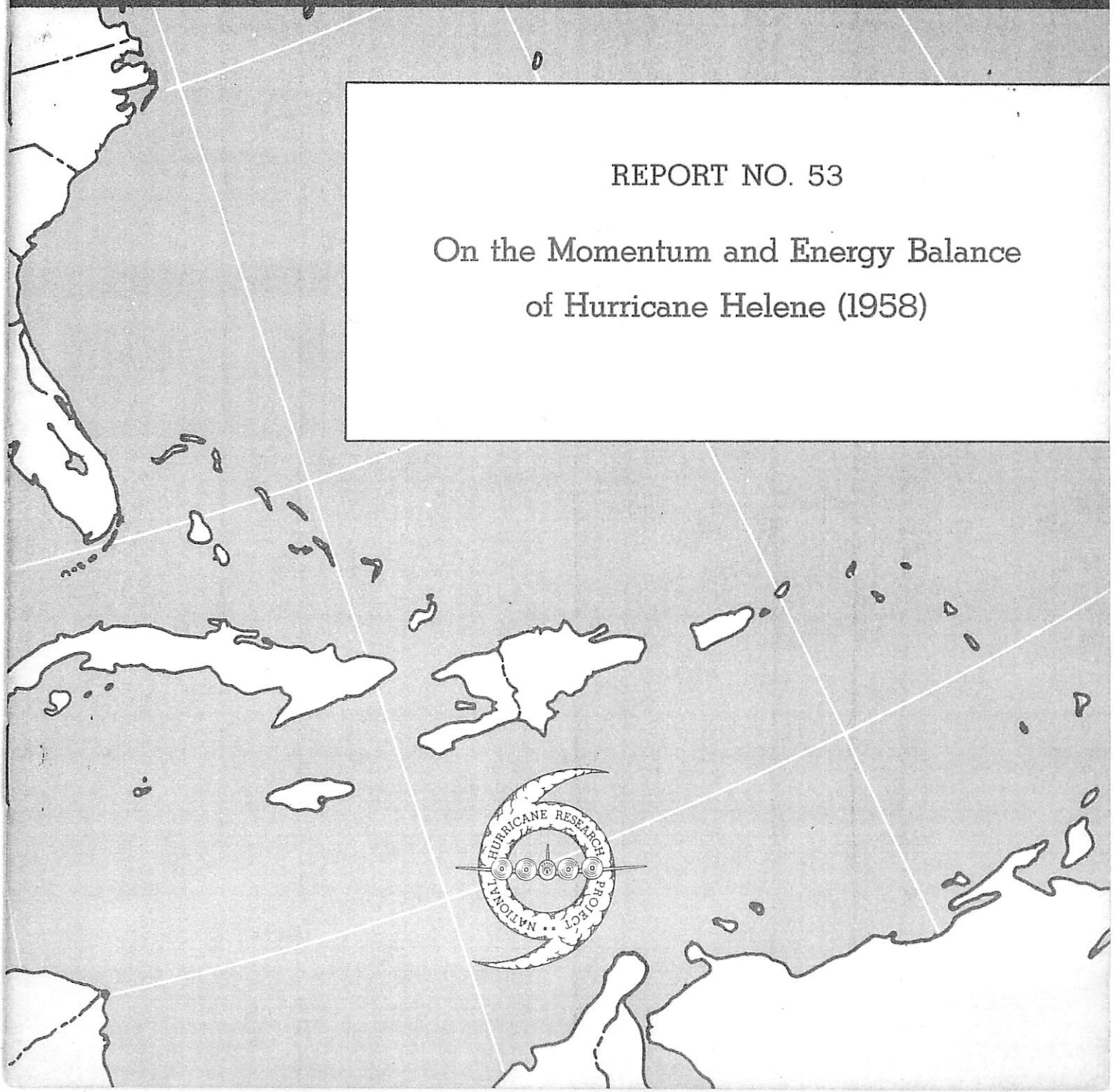

U. S. DEPARTMENT OF COMMERCE
Luther H. Hodges, Secretary
WEATHER BUREAU
F. W. Reichelderfer, Chief

NATIONAL HURRICANE RESEARCH PROJECT

REPORT NO. 53

On the Momentum and Energy Balance of Hurricane Helene (1958)

by

Banner I. Miller

National Hurricane Research Project, Miami, Fla.

Washington, D. C.
April 1962

NATIONAL HURRICANE RESEARCH PROJECT REPORTS

Reports by Weather Bureau units, contractors, and cooperators working on the hurricane problem are preprinted in this series to facilitate immediate distribution of the information among the workers and other interested units. As this limited reproduction and distribution in this form do not constitute formal scientific publication, reference to a paper in the series should identify it as a preprinted report.

No. 1. Objectives and basic design of the NHRP. March 1956.
No. 2. Numerical weather prediction of hurricane motion. July 1956.
Supplement: Error analysis of prognostic 500-mb. maps made for numerical weather prediction of hurricane motion. March 1957.
No. 3. Rainfall associated with hurricanes. July 1956.
No. 4. Some problems involved in the study of storm surges. December 1956.
No. 5. Survey of meteorological factors pertinent to reduction of loss of life and property in hurricane situations. March 1957.
No. 6. A mean atmosphere for the West Indies area. May 1957.
No. 7. An index of tide gages and tide gage records for the Atlantic and Gulf coasts of the United States. May 1957.
No. 8. Part I. Hurricanes and the sea surface temperature field. Part II. The exchange of energy between the sea and the atmosphere in relation to hurricane behavior. June 1957.
No. 9. Seasonal variations in the frequency of North Atlantic tropical cyclones related to the general circulation. July 1957.
No. 10. Estimating central pressure of tropical cyclones from aircraft data. August 1957.
No. 11. Instrumentation of National Hurricane Research Project aircraft. August 1957.
No. 12. Studies of hurricane spiral bands as observed on radar. September 1957.
No. 13. Mean soundings for the hurricane eye. September 1957.
No. 14. On the maximum intensity of hurricanes. December 1957.
No. 15. The three-dimensional wind structure around a tropical cyclone. January 1958.
No. 16. Modification of hurricanes through cloud seeding. May 1958.
No. 17. Analysis of tropical storm Frieda 1957. A preliminary report. June 1958.
No. 18. The use of mean layer winds as a hurricane steering mechanism. June 1958.
No. 19. Further examination of the balance of angular momentum in the mature hurricane. July 1958.
No. 20. On the energetics of the mature hurricane and other rotating wind systems. July 1958.
No. 21. Formation of tropical storms related to anomalies of the long-period mean circulation. September 1958.
No. 22. On production of kinetic energy from condensation heating. October 1958.
No. 23. Hurricane Audrey storm tide. October 1958.
No. 24. Details of circulation in the high energy core of hurricane Carrie. November 1958.
No. 25. Distribution of surface friction in hurricanes. November 1958.
No. 26. A note on the origin of hurricane radar spiral bands and the echoes which form them. February 1959.
No. 27. Proceedings of the Board of Review and Conference on Research Progress. March 1959.
No. 28. A model hurricane plan for a coastal community. March 1959.
No. 29. Exchange of heat, moisture, and momentum between hurricane Ella (1958) and its environment. April 1959.
No. 30. Mean soundings for the Gulf of Mexico area. April 1959.
No. 31. On the dynamics and energy transformations in steady-state hurricanes. August 1959.
No. 32. An interim hurricane storm surge forecasting guide. August 1959.
No. 33. Meteorological considerations pertinent to standard project hurricane, Atlantic and Gulf coasts of the United States. November 1959.
No. 34. Filling and intensity changes in hurricanes over land. November 1959.
No. 35. Wind and pressure fields in the stratosphere over the West Indies region in August 1958. December 1959.
No. 36. Climatological aspects of intensity of typhoons. February 1960.
No. 37. Unrest in the upper stratosphere over the Caribbean Sea during January 1960. April 1960.
No. 38. On quantitative precipitation forecasting. August 1960.
No. 39. Surface winds near the center of hurricanes (and other cyclones). September 1960.
No. 40. On initiation of tropical depressions and convection in a conditionally unstable atmosphere. October 1960.
No. 41. On the heat balance of the troposphere and water body of the Caribbean Sea. December 1960.
No. 42. Climatology of 24-hour North Atlantic tropical cyclone movements. January 1961.
No. 43. Prediction of movements and surface pressures of typhoon centers in the Far East by statistical methods. May 1961.
No. 44. Marked changes in the characteristics of the eye of intense typhoons between the deepening and filling states. May 1961.
No. 45. The occurrence of anomalous winds and their significance. June 1961.
No. 46. Some aspects of hurricane Daisy, 1958. July 1961.
No. 47. Concerning the mechanics and thermodynamics of the inflow layer of the mature hurricane. September 1961.
No. 48. On the structure of hurricane Daisy (1958). October 1961.
No. 49. Some properties of hurricane wind fields as deduced from trajectories. November 1961.
No. 50. Proceedings of the Second Technical Conference on Hurricanes, June 27-30, 1961, Miami Beach, Fla. March 1962.
No. 51. Concerning the general vertically averaged hydrodynamic equations with respect to basic storm equations. April 1962
No. 52. Inventory, use, and availability of NHRP meteorological data gathered by aircraft. April 1962.

CONTENTS

ON THE MOMENTUM AND ENERGY BALANCE OF HURRICANE HELENE (1958)

Banner I. Miller
National Hurricane Research Project, U. S. Weather Bureau,
Miami, Fla.

[Manuscript received August 8, 1961; revised September 11, 1961]

ABSTRACT

Using flight data supplemented by surface ship observations, the vertical fluxes of angular momentum, kinetic energy, sensible and latent heat are calculated for hurricane Helene (1958). These computations are used to estimate the surface exchange coefficients at various radii. Although the accuracy of the data makes the results questionable, it is found that the coefficient for heat and moisture exchange is about 1.3 times that for angular momentum. From the kinetic energy budget, internal frictional dissipation is obtained as a residual. In the wall cloud region it is found that internal friction exceeds the ground friction, but that elsewhere in the cyclone the two are about equal. The importance of internal friction in determining the heat balance is discussed briefly.

1. INTRODUCTION

Several attempts have been made to obtain a detailed picture of the circulation of a tropical cyclone by compositing data [3, 4, 8] from several different cyclones. Palmén and Riehl [10] have used some of these data to compute the budgets of angular momentum, kinetic energy, and heat. Such studies have contributed to our understanding of the mechanisms of hurricanes, but they leave much to be desired for several reasons.

First, the compositing process may very well obscure some important features of the cyclone, and it appears unlikely that the "mean cyclone" is ever observed in nature. Whether the individual variations of tropical cyclones are important, or just "noise," cannot be determined at this time. Second, the mean data are biased or incomplete in the high energy core of the cyclone, and calculations have to be extrapolated into this region or omitted altogether. This is unsatisfactory, because it is this inner region which holds the most interest and importance for the meteorologist.

Recent airplane observations made by the National Hurricane Research Project in the high energy core of several hurricanes have provided sufficiently detailed data to permit calculations of angular momentum, kinetic energy, etc., within the inner region. Riehl and Malkus [11] have performed such calculations for hurricane Daisy (1958). In spite of some uncertainties in the data, these computations have shed considerable light on the internal hurricane mechanisms. Comparable flight data exist for hurricane Helene (1958), and it is the purpose of this paper to carry out calculations of a similar nature for the latter cyclone. A comparison between the two hurricanes should be of interest, and when a series of such calculations is available, it may be possible to improve existing hurricane models and to determine whether or not the anomalous features of individual cyclones are of fundamen-

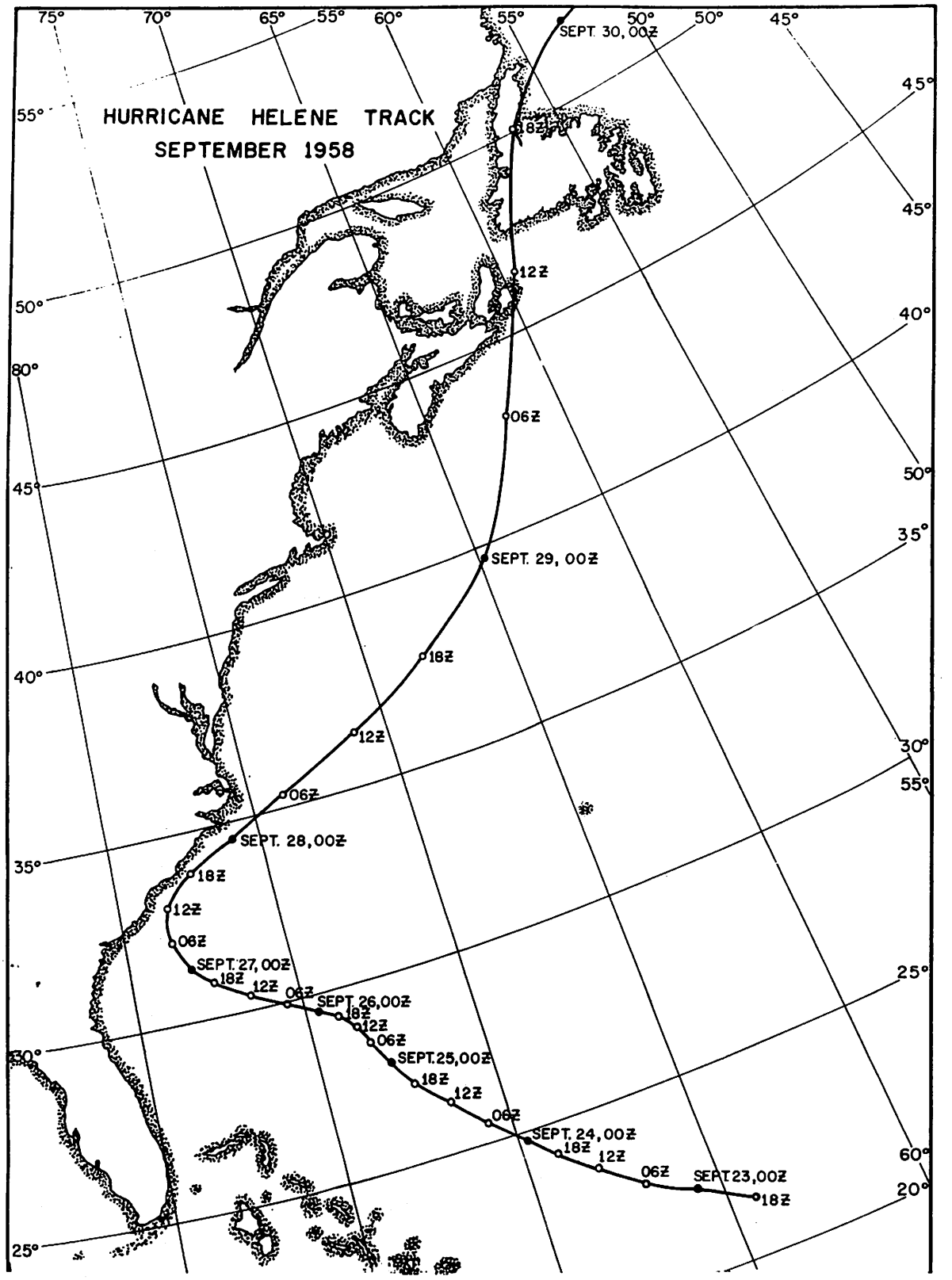

Figure 1. - Track of hurricane Helene, September 1958.

tal importance. One must keep in mind, however, that conclusions based on calculations such as these must be regarded as tentative, and that they may have to be revised as new cases are analyzed.

Hurricane Helene [14] developed from an easterly wave, which could be tracked as far back as the Cape Verde Islands. Intensification began on September 20 northeast of the Windward Islands. By the 24th the cyclone had reached hurricane intensity; at that time it was located north of the central Bahamas (fig. 1). It reached its maximum intensity (lowest central pressure) about 0500 GMT on the 27th when it was located off the Carolina coast. Lowest recorded central pressure, by dropsonde, was about 933 mb. Rapid intensification occurred on the 26th, as shown by the pressure profile in figure 2. By late afternoon of the 26th, however, maximum intensity had almost been

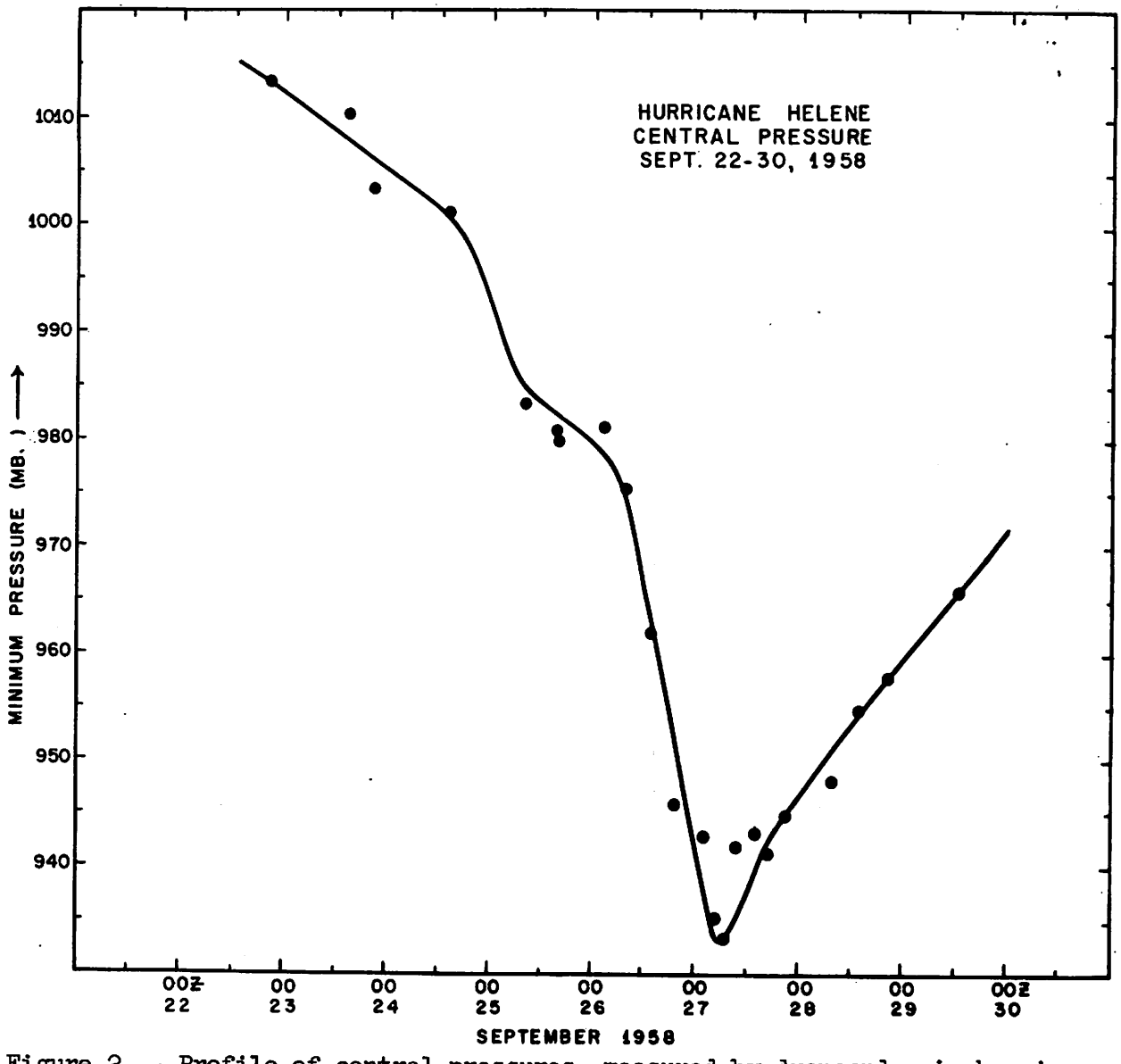

Figure 2. - Profile of central pressures, measured by dropsonde, in hurricane Helene, September 1958.

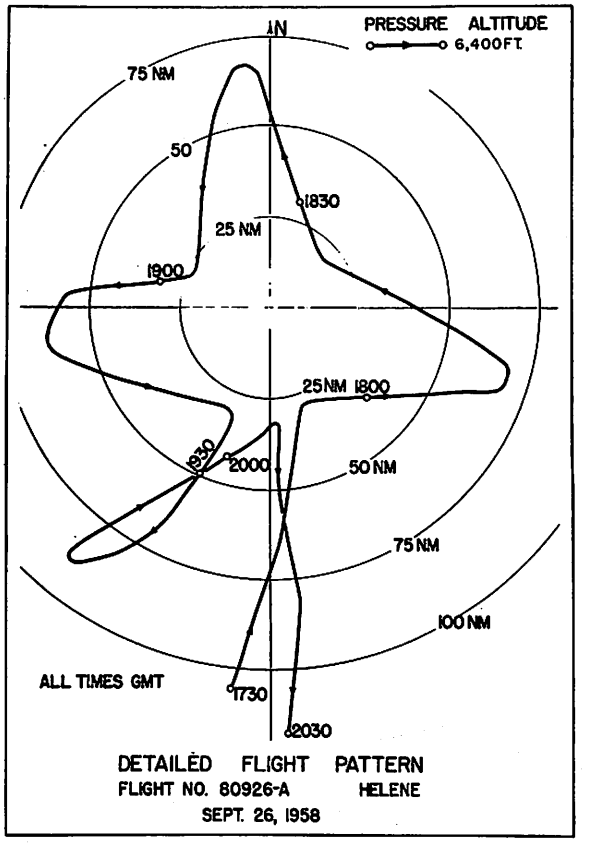

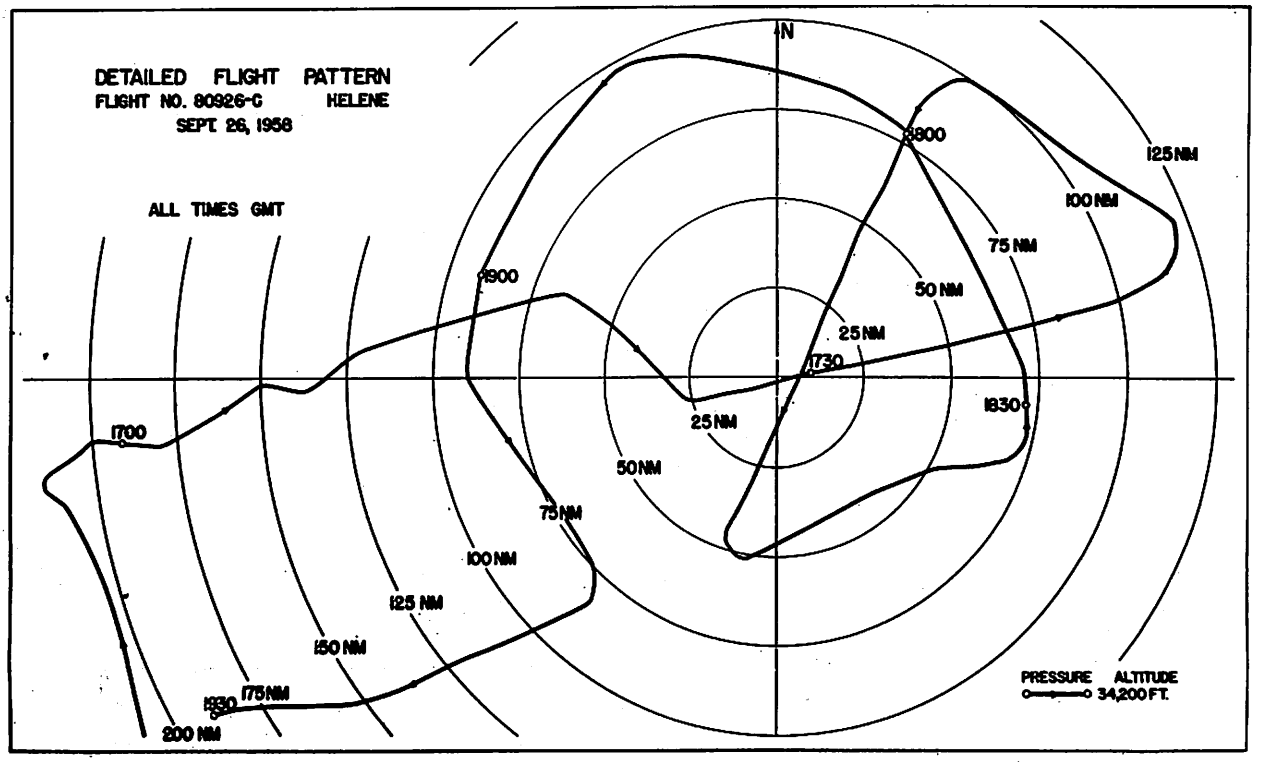

Figure 3. - Flight paths of NHRP aircraft on September 26: (a) at 800 mb., (b) at 237 mb.

reached. Flight data to be analyzed were collected on the afternoon of the 26th; calculations to be performed will, therefore, be based on the assumption that a steady state had been reached.

On the 25th, NHRP flew tracks at 1600 ft. and 6400 ft. There were no flights at any higher level. Consequently, computations of energy and momentum balance could not be carried out. These flights, however, were useful in establishing the low-level mass flow.

On the 26th NHRP aircraft flew extensive tracks at 800- and 237-mb. levels, as shown in figure 3. Measurements of wind, temperature, and "D" values were made at both levels. In addition, relative humidity was measured at the lower level. Limited tracks (essentially radial passes) were also flown on the 26th at 700 mb. and 560 mb. The latter were useful in establishing radial profiles of "D" value, temperature, and relative humidity, but they could not be used to evaluate the radial or tangential wind components. Surface ship observations, composited with respect to the cyclone center, supplemented the aircraft data on both the 25th and 26th.

2. MASS FLOW

Since there were no upper tropospheric reconnaissance flights on the 25th and no circumnavigation of the cyclone center below the 800-mb. level on the 26th, determination of the mass flow presented more than the usual amount of difficulty. The radial wind components computed from the aircraft observations were somewhat erratic and it was not possible to construct a reasonably accurate isotach pattern from these data. Consequently, the mass flow as finally determined is subject to more than the normal amount of doubt attached to such computations. The procedure used was as follows:

1. To obtain the low-level mass flow, data from surface ships were composited with respect to the cyclone center on both the 25th and the 26th. On both days it was necessary to composite the ship data for the entire 24-hour period in order to obtain a usable sample. A shorter period centered around the respective flight times would have provided a more compatible value for the mass flow, since the hurricane deepened greatly on both days (fig. 3). From the composite data $\bar{v}_r$ was calculated: however, as usual there were few ships inside a radius of about 2° of latitude.

2. On the 25th it was possible to supplement the ship data with flight observations made at 1600 ft. (960 mb.). This flight circumnavigated the center at an average distance of about 65 n.mi., thus providing a point on the mass flow diagram at that radius (fig. 4). A smooth curve was then drawn with the mass flow assumed to decrease linearly inside the 60 n.mi. radius to the eye wall, which was near the 15 n. mi. radius.

3. On the 26th surface ship data were treated in the same manner as on the 25th. There was no low-level reconnaissance flight to supplement the ship data. To obtain an estimate of the mass flow, it was assumed that the mass flow curve had the same general shape on the 26th as it had on the 25th. A smooth curve was drawn (fig. 4). This curve shows that the mass flow was

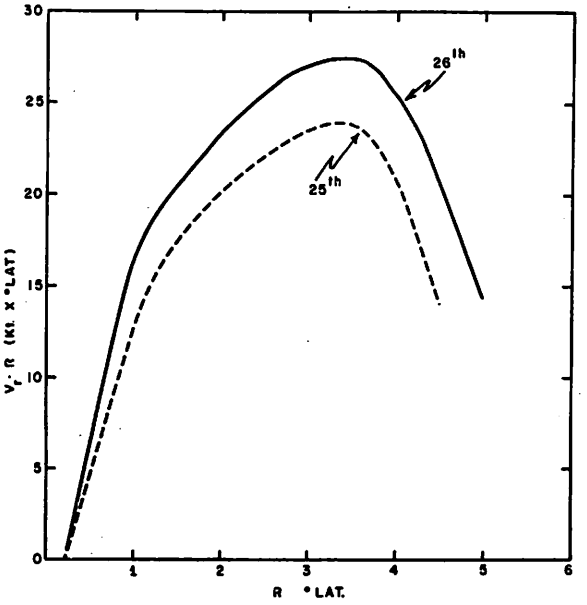

Figure 4. - Surface mass flow, September 25 and 26, 1958.

greater on the 26th than it was on the 25th, in agreement with the work of Krueger [6], who found a linear correlation between mass flow and central pressures in hurricanes.

4. At the flight levels, the radial wind components were somewhat erratic and no satisfactory analysis could be performed. Instead of computing radial components, it was decided to compute the wind component normal to the flight path, thus eliminating the necessity for drawing isotachs. Normal wind components were computed for every wind observation, and a smooth curve was drawn through these values. The average value for v_n was obtained, and since the flight path circumnavigated the center, it was assumed that $\bar{v}_r$ was equal to $\bar{v}_n$. This value of $\bar{v}_r$ was assigned to a radius equal to the mean distance of the flight path from the center. This corresponded to about 55 n. mi. at 800 mb. and about 70 n. mi. at 237 mb. Both values were then adjusted to their equivalents at 60 n. mi. radius for convenience in performing the computations. This was done by assuming linear variation of mass flow with radius. Inner values at 40- and 20-n.mi. radii were also obtained by assuming linear decrease in the mass flow from 60 n.mi. to 15 n.mi., the radius of the eye wall. Values are tabulated in table 1.

5. Mass balance was then obtained in the usual manner by setting

$$\int_{p_o}^{p_h} v_r \, dp = 0 \qquad (1)$$

where p_o is the surface and p_h is the pressure at the top of the cyclone (about 100 mb.). Vertical profiles of mass flow are shown in figure 5. These profiles represent the simplest curves which could be drawn to obtain mass balance, but it should be emphasized that they are not uniquely determined.

Table 1. $\bar{v}_r$ (knots) at various radii and pressures on September 26,1958.

Radius (n.mi.)	960 mb.	800 mb.	237 mb.
60	-17.0	-2.2	11.5
40	-14.4	-1.9	9.5
20	- 6.2	-0.8	4.0

It is of interest that these profiles show no mass inflow between 700 mb. and 400 mb. There was actually a decrease in the mass inflow at 800 mb. between the 25th and the 26th, during

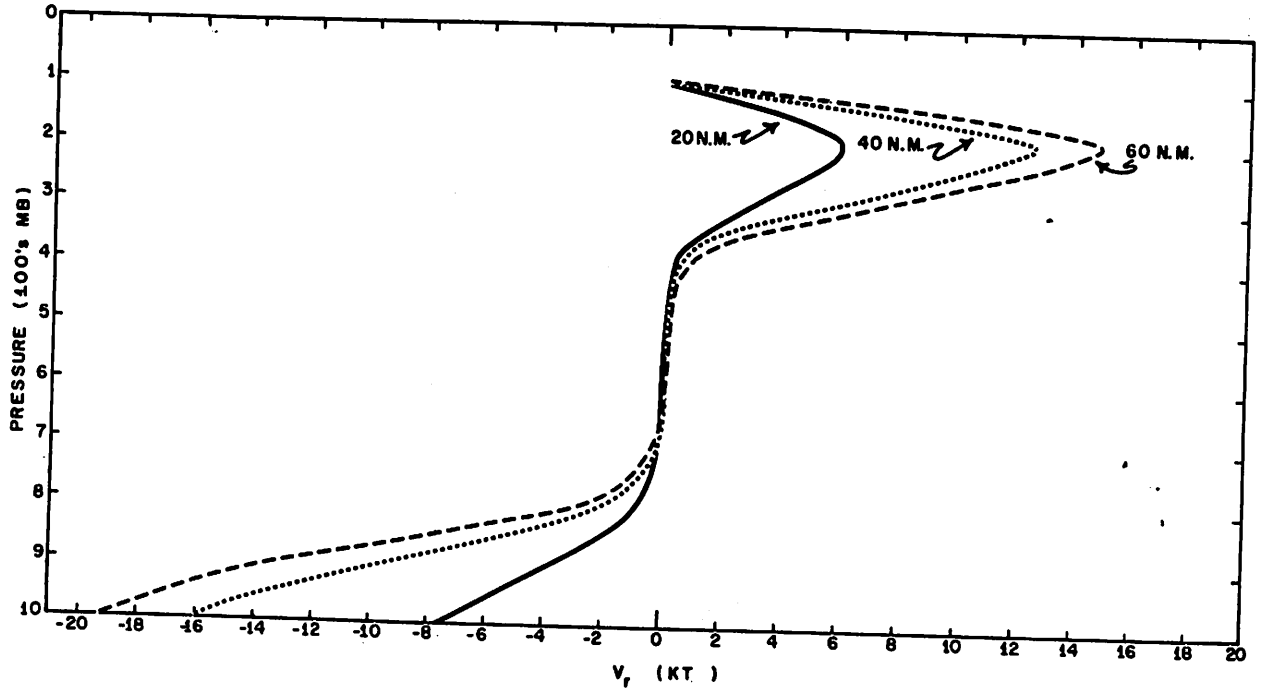

Figure 5. - Vertical profiles of radial winds, September 26.

which time the cyclone deepened more than 40 mb. While it is admitted that the deep layer of no inflow is somewhat questionable, it does, if accepted, indicate a lack of mid-tropospheric cooling, termed "ventilation" by Riehl and Simpson [13], and this absence is consistent with the strong deepening actually observed to occur. In contrast, inflow was observed in hurricane Daisy up to about 500 mb. [11], indicating that active ventilation was at work. Daisy was a smaller and less intense cyclone than Helene. Consequently the absence of mid-tropospheric inflow in Helene is probably acceptable.

Due to the manner in which the radial wind components were determined, it was not possible to compute radial transports due to the eddy motion. This fact should be kept in mind in evaluating the computations which follow.

3. ANALYSIS OF OTHER FLIGHT DATA

Tangential wind profiles were obtained from isotach analysis of the v_θ components at the 800- and 237-mb. flight levels. Mean values were computed for radial intervals of 10 n.mi. by averaging twelve values at 30° intervals. To obtain a vertical profile, it was assumed that the tangential wind approached zero at 100 mb. and that v_θ was virtually constant below 500 mb. Both these assumptions are adequately supported by flight observations of other cyclones [1] and by composite data [4,8]. Vertical profiles of v_θ are shown in figure 6.

The 800-mb. level winds were used as a representation of the surface winds, which were needed to compute the surface frictional dissipation of

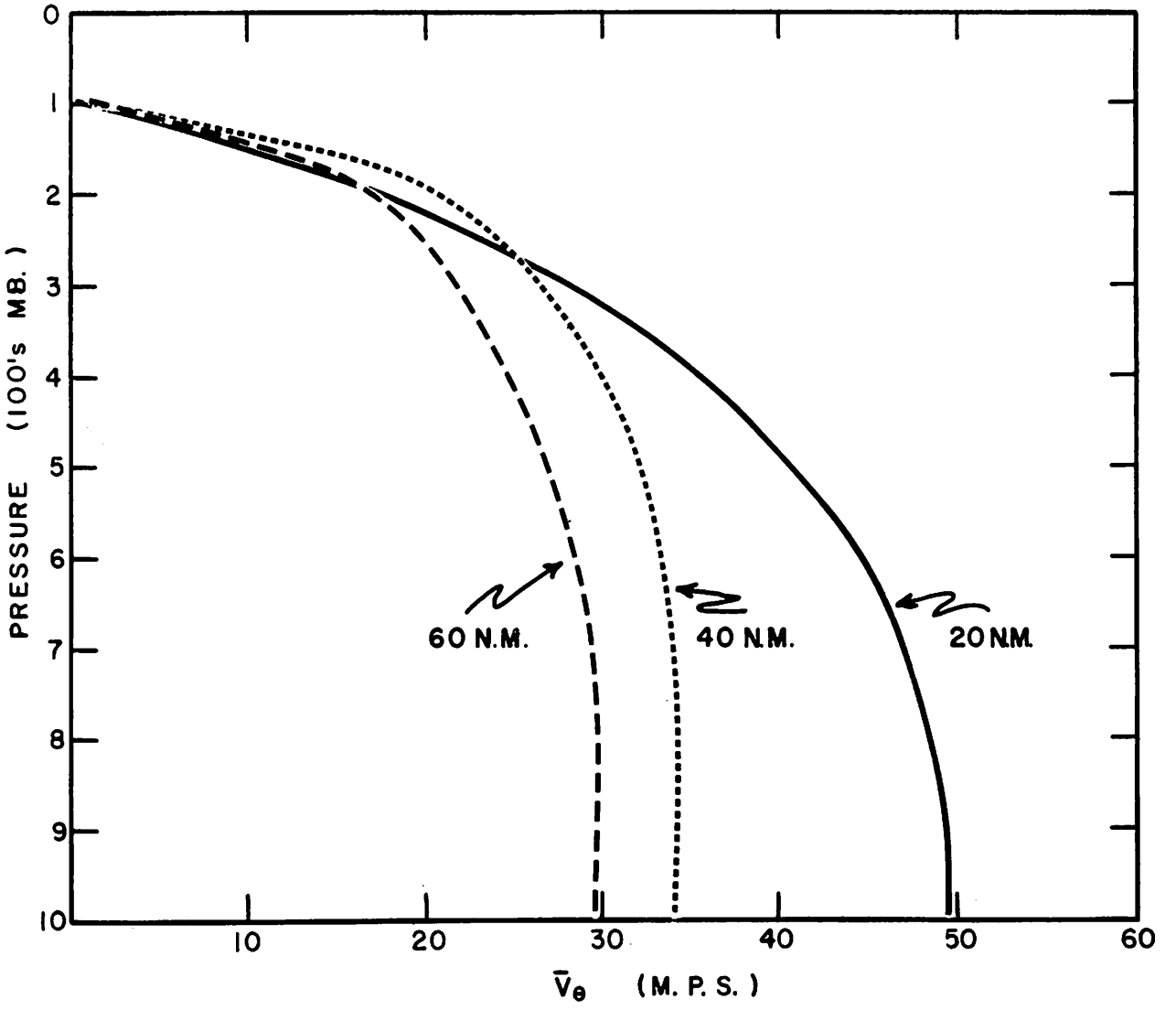

Figure 6. - Vertical profiles of tangential winds, September 26.

kinetic energy and the heat fluxes from the ocean to the atmosphere. The profile of figure 7 was based on the 800-mb. level, with the exception of the portion inside the eye, which was based on a radial pass at 700 mb. The 800-mb. flight did not penetrate the eye (fig. 3), and consequently the maximum wind was probably not encountered. Actual highest measured wind at 800 mb. was 99 kt. at a radius of about 20 n.mi. The maximum wind at the 15 n.mi. radius is an extrapolated value, based on a $v_n^{0.54}$ constant profile. The value of 0.54 was determined from the wind profile between the 20 and 60 n.mi. radii.

The vertical distributions of temperature, mixing ratio, and "D" values were also obtained by using the mean radial values at 800 and 237 mb. as "anchor positions," to which were added points at the surface, 700, 500, 560, and 100 mb., based on the following procedures:

1. Generally sea and air temperatures at the surface were not available within the 60 n.mi. radius, the main area of interest. By compositing the data from all available surface ships within a 2° to 4°lat. ring, mean values of sea and air temperature were found to be 28.7° and 27.8°C., respectively. The mean pressure at these radii was about 1015 mb. If adiabatic expansion from the pressure to 1000 mb. (which occurred at about the 60 n.mi. radius) takes place, a cooling of slightly more than 1° would occur. It was assumed that the temperature of the ocean remained approximately constant inside the 2° lat. radius, and, consequently, it was deemed plausible to use a constant sea-air difference at 2°C., a value suggested by Malkus and Riehl [7]. Mixing ratio was estimated by assuming a linear increase in relative humidity from 85 percent at the 60 n.mi. radius to 95 percent at the eye wall.

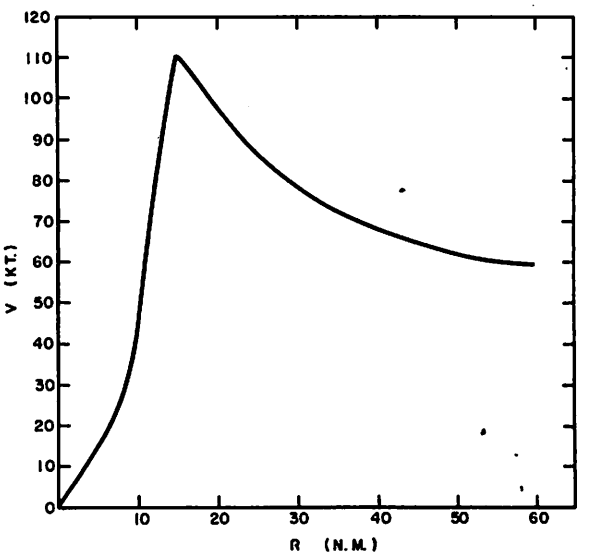

Figure 7. - Radial profile of total wind speed, based on 800- and 700-mb. data.

2. A vertical sounding was constructed for the eye, using dropsonde data below 700 mb., aircraft measurements at 560 and 237 mb., and an assumed lapse rate of 8°C. per km. above 237 mb. This sounding terminated in a temperature of -73°C. at the 100-mb. level.

3. Vertical soundings were constructed at the 20-, 40-, and 60-n.mi. radii, using the surface data described under (1) above, mean values at 800 and 237 mb., radial passes at 700 and 560 mb., and an assumed lapse rate above 237 mb. chosen so as to result in a constant temperature of -73°C. at 100 mb. inside the 60 n.mi. radius.

4. Above 560 mb. there were no humidity measurements and outside the eye it was assumed that the relative humidity was 90 percent of saturation.

5. Soundings were checked for vertical consistency by computing the thicknesses of 100-mb. layers indicated by the mean virtual temperatures. Using these thicknesses, heights of the standard constant pressure surfaces were computed, starting with the central pressure as measured by a dropsonde inside the eye and the "D" value profile at the 800-mb. level. Computed heights were then compared with the heights measured by aircraft and dropsonde. Some minor adjustments were required in the contructed soundings in order to achieve hydrostatic consistency. These were mainly an adjustment of less than 1°C. in the 700-mb. temperature at the 60 n.mi. radius and in the assumed lapse rate above 237 mb.

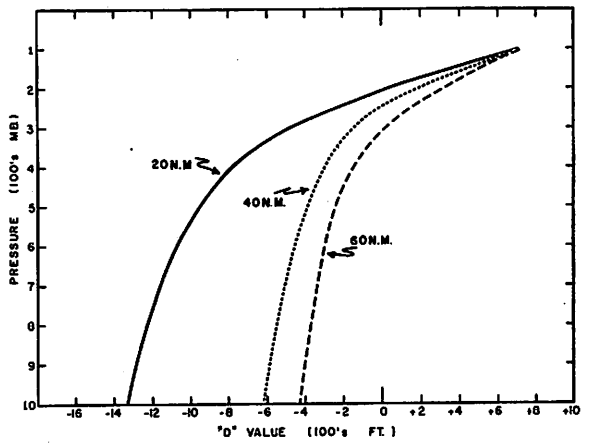

Figure 8. - Vertical profiles of "D" values, deviations in 100's feet from mean tropical atmosphere.

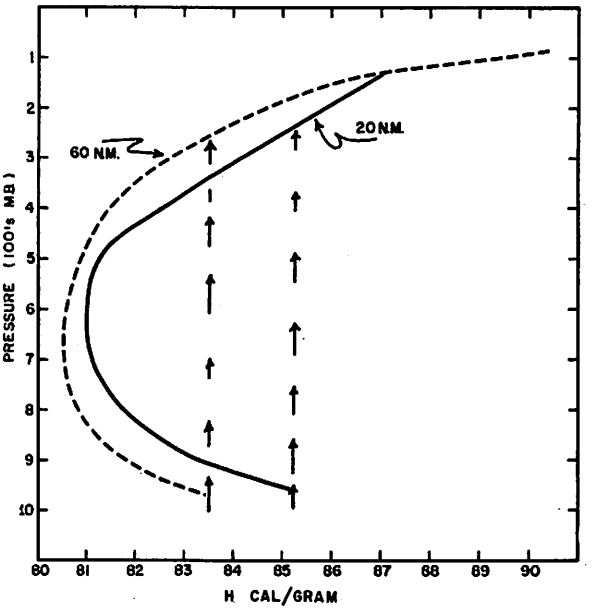

Figure 9. - Vertical distributions of H at 20 and 60 n.mi. radii.
$H = gz + c_pT + Lq$,(cal./gr.)

6. Vertical profiles of "D" values and H were then constructed. The "D" values are the differences between the actual constant pressure heights and the heights indicated by the tropical standard atmosphere [5]. H is defined as

$$H \equiv c_pT + gz + Lq \tag{2}$$

where c_p is the specific heat of air at constant pressure, T is the absolute temperature, L is the heat of condensation, q is mixing ratio, g is the acceleration of gravity, and z is the height of the constant pressure surface. Profiles of "D" and H are shown in figures 8 and 9. These will be used in subsequent calculations of kinetic and other energy balances.

4. ANGULAR MOMENTUM

The absolute angular momentum, M, per unit mass of air, expressed in a cylindrical coordinate system, is

$$M = v_\theta r + \frac{fr^2}{2} \tag{3}$$

where f is the Coriolis parameter, other symbols having been defined earlier. The tangential equation of motion may be transformed into a momentum equation, resulting in

$$\frac{dM}{dt} = -\frac{1}{\rho}\frac{\partial p}{\partial \theta} + \frac{r}{\rho}\left(\frac{\partial \tau_{\theta\theta}}{r\partial\theta} + \frac{\partial r\,\tau_{\theta r}}{r\partial r} + \frac{\partial \tau_{\theta z}}{\partial z}\right) \tag{4}$$

where τ_{ij} refers to the shearing stresses.

Equation (4) states that the change in absolute angular momentum of a parcel of air is the result of production by pressure forces and dissipation due to friction. Integration of (4) over the volume of the cylinder yields

$$\frac{\partial}{\partial t}\int_{\alpha}\rho M d\alpha = \int_{p_2}^{p_1}\int_{0}^{2\pi} v_r\left(v_\theta r + \frac{fr^2}{2}\right) r d\theta \frac{dp}{g}$$

$$- \int_{\alpha}\frac{\partial p}{\partial \theta} d\alpha + \int_{\alpha} r\left(\frac{\partial \tau_{\theta\theta}}{r\partial\theta} + \frac{\partial r\tau_{\theta r}}{r\partial r} + \frac{\partial \tau_{\theta z}}{dz}\right) d\alpha \qquad (5)$$

in which it has been assumed that f is a constant. For an axially symmetric cyclone, the production term vanishes. The lateral exchange of angular momentum by small-scale stresses (the first two terms in the third integral on the right) are in general considered to be small in comparison with the vertical transport term. This may not be true near the eye wall, but at any rate lateral transports cannot be evaluated with present data and knowledge of the lateral exchange coefficients. Consequently, lateral transport will be neglected. With the further assumption of steady state conditions, equation (5) becomes

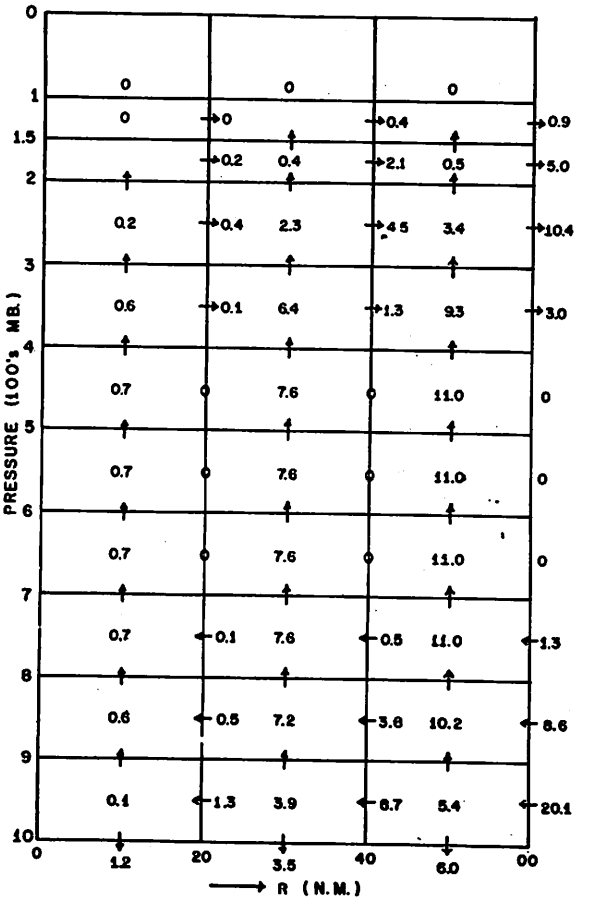

Figure 10. - Flux of angular momentum. Units of 10^{22} g.cm.^{2}sec.$^{-2}$.

$$\int_{p_2}^{p_1}\int_{0}^{2\pi} v_r\left(v_\theta r + \frac{fr^2}{2}\right) r d\theta \frac{dp}{g} + \int_{\alpha} r\frac{\partial \tau_{\theta z}}{\partial z} d\alpha = 0 \qquad (6)$$

The integration of the momentum transport was carried out for 100-mb. layers and radial intervals of 20 n.mi. Only the transport due to the mean motion could be calculated. Riehl [12] has shown that the eddy transport of angular momentum is small compared to the transport by the mean motion. Hence the resulting calculations are probably reasonable. The momentum fluxes are shown in figure 10.

With the assumptions implicit in equation (6), the net divergence of momentum must equal the transfer to the ocean surface [10]. The torque exerted on the ocean is then

$$M_o = 2\pi \int_{r_1}^{r_2} \overline{\tau}_{\theta o} \, r^2 dr \tag{7}$$

where $\overline{\tau}_{\theta o}$ is the mean tangential surface stress between the two radii. By making use of the empirical formula

$$\tau_{\theta o} = \rho \, c_d \, v_o \, v_{\theta o} \tag{8}$$

where c_d is a non-dimensional drag coefficient, and v_o and $v_{\theta o}$ are the surface wind and its tangential component, the drag coefficient may be computed as a function of the radius or the surface wind velocity. Thus

$$c_d = \frac{M_o}{2\pi\rho_o \int_{r_1}^{r_2} \overline{v_o \, v_{\theta o}} \, r^2 dr} \tag{9}$$

The results of these computations of c_d are shown in table 2.

Palmén and Riehl [10] computed drag coefficients from the mean hurricane data of Hughes [3] and E. Jordan [4]. They obtained values ranging from 1.1 x 10^{-3} to 2.1 x 10^{-3} for wind velocities of 6 to 26 m.p.s. Their computations were also made by use of the angular momentum budget. It is of interest that in spite of the crudeness of the Helene calculations, they represent an almost linear extension of the Palmén-Riehl values when c_d is plotted against the surface wind velocity.

In the case of hurricane Daisy, Riehl and Malkus [11] have used an assumed drag coefficient of 2.5 x 10^{-3}, taken as constant inside the 80 n.mi. radius, for use in estimating the transfer of angular momentum to the ocean. Using this procedure, they found that on the 25th of August (when Daisy was still in the tropical storm stage), the balance of angular momentum can be very nearly achieved without making any allowances for the transfer by lateral stresses. On the 27th, however, when Daisy was at maximum intensity, it was necessary to invoke a sizable export due to lateral stresses in order to

Table 2. - Drag coefficients and tangential surface stresses computed from the angular momentum balance.

Radius	0-20 n.mi.	20-40 n.mi.	40-60 n.mi.
c_d x 10^3	3.2	2.7	2.4
$\overline{\tau}_{\theta o}$ (dynes/cm.^{2})	60.0	51.0	27.6

achieve balance. They found that only about one-half the total angular momentum imported by the mass circulation was transferred to the ocean surface. Should a similar situation have existed in the case of Helene on September 26, the drag coefficients computed by the use of equation (9) would have to be materially reduced. Alternately, if later developments should show that the lateral exchange of momentum is less than that found for Daisy on August 27, it could be argued with equal logic that Riehl and Malkus used too low a value for the drag coefficients on the 27th. This would then indicate that the use of drag coefficients as a function of surface wind speed, as indicated by the Palmén-Riehl and Helene calculations, is appropriate. The latter is probably correct, but such dependence cannot now be placed on any sort of firm basis. The uncertainty points to the urgent need for an adequate observational program for the determination of both surface and lateral exchange coefficients.

5. KINETIC ENERGY

For a fixed volume in the atmosphere the rate of change of kinetic energy may be expressed by

$$\frac{\partial}{\partial t}\int_{\alpha} \rho K \, d\alpha = -\int_{p_o}^{p}\int_{A} K v_n \, dA \frac{dp}{g} - \iiint \mathbf{V} \cdot \nabla h dA dp + \int_{\alpha} \rho \mathbf{V} \cdot \mathbf{F} d\alpha \qquad (10)$$

where K is the kinetic energy per unit volume, v_n is the velocity normal to the boundary, α is a unit of volume, ρ is the density, dA is an element of area, h is the height of the constant pressure surface, $\mathbf{F}$ is the friction, and $\mathbf{V}$ is the wind velocity. The first integral on the right indicates the advection of kinetic energy through the boundary, the second is the production by pressure forces, and the third the dissipation due to friction, both surface and internal.

The advection term is easily computed from the mass flow and the vertical profile of the total wind speeds. For an axially symmetrical pressure height field, the production may be written (neglecting the kinetic energy of vertical motion)

$$\iiint v \cdot \nabla h dA dp = \int v_r \frac{\partial h}{\partial r} dA dp \qquad (11)$$

and this may be evaluated from the vertical profiles of radial winds and "D" values (figs. 5 and 8). The dissipation may be divided into that due to ground friction and internal friction. The former may be expressed by the formula (7)

$$\text{G. F.} = \int_{A} c_d \rho_o v_o^3 \, dA \qquad (12)$$

Table 3. - Kinetic energy budget September 26 (upper numbers) compared to hurricane Daisy on August 26 (lower numbers, taken from Riehl and Malkus [11]). Units of 10^{14} kj/day.

Radial interval (n.mi.)	0-20	20-40	40-60	0-60
Advection	0.9 / 1.6	0.6 / 1.0	0.6 / 0.7	2.1 / 3.3
Production	0.9 / 1.0	3.6 / 2.0	2.4 / 1.5	6.9 / 4.5
Dissipation due to surface friction	0.7 / 0.6	2.1 / 0.8	1.6 / 0.7	4.4 / 2.1
Advection plus production	1.8 / 2.6	4.2 / 3.0	3.0 / 2.2	9.0 / 7.8
Left over for internal friction	1.1 / 1.9	2.1 / 2.1	1.4 / 1.4	4.6 / 5.4
Ratio of internal friction to ground dissipation	1.6 / 3.2	1.0 / 2.6	0.9 / 2.0	1.0 / 2.6

Internal friction cannot be evaluated directly due to lack of information concerning exchange coefficients and the uncertainties associated with the vertical and horizonal variations of the wind. Under steady state conditions, however, internal friction may be calculated as a residual from equations (8-10).

The production term was evaluated from equation (9) after preparation of $\frac{\partial \tilde{h}}{\partial r}$ and $\tilde{v}_r$ for 100-mb. layers, using the data of figures 5 and 8. The advection term was evaluated from the mass flow. Riehl and Malkus [11] found that the eddy term may be as much as 25 percent of the mean term. Since the eddy term could not be determined, the results of the kinetic energy transport calculations may be in error by at least that amount. The dissipation due to surface friction was evaluated from equation (10), using the drag coefficients computed from the angular momentum budget and the wind profile of figure 7. The results of these calculations are summarized in table 3.

A comparison with the results of similar computations for Daisy [11] shows that even though Helene had stronger winds and covered a larger area than Daisy, advection of kinetic energy into the hurricane core was larger in Daisy than in Helene. This is probably due to the fact that the inflow was much deeper in Daisy than in Helene. However, both production and surface dissipation of kinetic energy were much greater within the 20-60 n.mi. ring in Helene than in Daisy, reflecting the stronger surface winds and pressure gradients. Of major interest is the fact that the amount of kinetic energy left over for internal friction was almost identical in the two cyclones.

6. HEAT BALANCE

The flux divergence of H, as defined by equation (2), may be written

$$\text{Div } H = \int_{p_o}^{p_H} \int_{0}^{2\pi} (gz + c_p T + Lq)\, v_r \, ds \, \frac{dp}{g} \tag{13}$$

and this quantity can be calculated from the mass flow and the vertical profile of H (figs. 5 and 9). Under steady state conditions one may also write

$$Q_a = \text{Div } H + R_a \tag{14}$$

where Q_a is the total heat source and R_a is the net outgoing radiation. Q_a consists of two parts, Q_s, the sensible heat, and Q_e, the latent heat, both of which are supplied by the ocean surface. If the results of the calculations of internal friction, described earlier, are eventually verified, it may be necessary to add a third term to Q_a, i. e. Q_k, where the latter is defined as the heat equivalent of internal friction.

The vertical fluxes of latent and sensible heat may be calculated from

$$Q_s = c_p \rho c_h (\widetilde{T_o - T_a})\, v A \tag{15}$$

$$Q_e = \rho L c_e (\widetilde{q_o - q_a})\, v A \tag{16}$$

Here the wavy bar "$\sim$" indicates an areal average, c_h and c_e are non-dimensional exchange coefficients for heat and moisture, T_o and q_o are the temperature and saturation mixing ratio of the ocean surface, while T_a and q_a are the temperature and actual mixing ratio of the air, v is the wind speed, and A is the area.

As a first approximation, Q_s and Q_e were computed by assuming that c_h and c_e are equal to c_d and then using the values for c_d obtained from the angular momentum budget. Later c_h and c_e were computed separately and the new values compared with those for c_d.

The results of these calculations are shown in figure 11. Balance is not quite achieved. The indicated export exceeds the available heat by 1.5 units, without making any allowance for loss by radiation. By adding the heat equivalent of internal friction, Q_k, to the source, this excess is reduced to 0.1 unit, which still leaves nothing left over for radiation. The results are summarized in table 4.

Table 4. - Total heat budget, September 26, units 10^{12} cal./sec. Q_k is heat equivalent of internal friction.

Radial interval (n. mi.)	0-20	20-40	40-60	0-60
Q_a + Div H	+0.2	+0.5	+0.8	+1.5
Q_k	-0.3	-0.6	-0.5	-1.4
Total	-0.1	-0.1	+0.3	+0.1

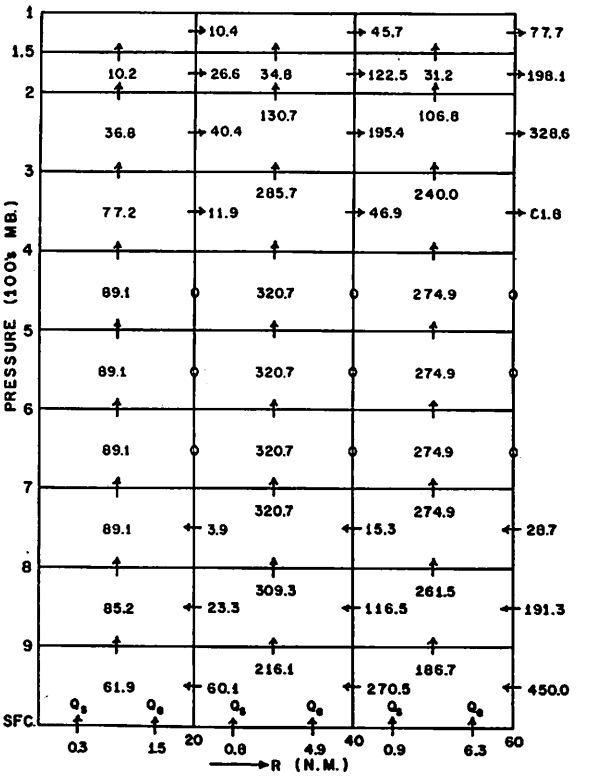

Figure 11. - Divergence of H, plus Q_a, units of 10^{12} cal./sec. $Q_a = Q_s + Q_e$, where Q_s and Q_e are vertical fluxes of sensible and latent heat. H is defined as in figure 9.

Further attempts to achieve complete balance, with proper allowance for radiation, seem futile, since the imbalance is almost certainly exceeded by the eddy transports, which could not be evaluated. Balance could be achieved by slight adjustment in H or $\bar{v}_r$ at any one of several levels, and such adjustment would certainly be within the limits of observational errors. We can, however, inquire as to values of c_h and c_e required to produce balance, assuming that Div H is correct.

The exchange coefficients for heat and moisture may be computed by assuming that c_h and c_e are equal (there is no physical reason for them to differ) and then making use of the Bowen ratio, defined by

$$r_B = \frac{c_p}{L}\frac{T_o - T_a}{q_o - q_a} = \frac{Q_s}{Q_e} \qquad (17)$$

Q_a is defined as the sum of Q_s and Q_e. Losses by radiation are computed by assuming black body radiation at a temperature equivalent to that at the top of the heavy cirrus cloud deck, or about -40°C. Q_a is then determined from equation (14); hence Q_s and Q_e as well as the required values for c_h and c_e can be determined. Results are listed in table 5.

Table 5. - Summary of calculation of exchange coefficients from heat budget.

Radial interval	0-20 n.mi.	20-40 n.mi.	40-60 n.mi.
$T_o - T_a$ (°C.)	2.0	2.0	2.0
$q_o - q_a$ (g./kg.)	4.4	4.7	5.9
v (m.p.s.)	40.4	38.8	31.0
r_b	.19	.18	.15
$Q_s \times 10^{-12}$ cal./sec.	0.35	1.0	1.14
$Q_e \times 10^{-12}$ cal./sec.	1.85	5.7	7.66
$R_a \times 10^{-12}$ cal./sec.	0.2	0.5	0.8
$c_h = c_e \times 10^3$	3.6	3.5	3.2
c_h/c_d	1.1	1.3	1.3

The main feature of interest in table 5 is that the heat budget can be balanced by using values for c_e and c_h slightly in excess of those used for c_d. The actual ratio of c_h/c_d is 1.3 in the 20-60 n.mi. ring, slightly less inside the 20 n.mi. radius. This value, 1.3, is almost exactly the expected ratio of K_m/K_h (eddy viscosity to eddy conductivity) for the lower limits of free convection, as indicated by Ellison [2], Taylor [15], Panofsky et al. [9]. It is perhaps more than coincidence that this ratio should be found in tropical cyclones, although the crudeness of the computations makes it impossible to attach any real significance to this result. It should also be pointed out that if Q_k (heat equivalent of internal friction) is included as a part of Q_a, the values for c_h and c_e are reduced slightly.

7. TOTAL MOISTURE AND RAINFALL RATES

The divergence of moisture may be used to estimate the probable rainfall associated with hurricane Helene. The results of a separate determination of the moisture budget are shown in figure 12. Converted to precipitation, the divergence of moisture is equivalent to the amounts listed in table 6. These values are well within the range of expected values [3].

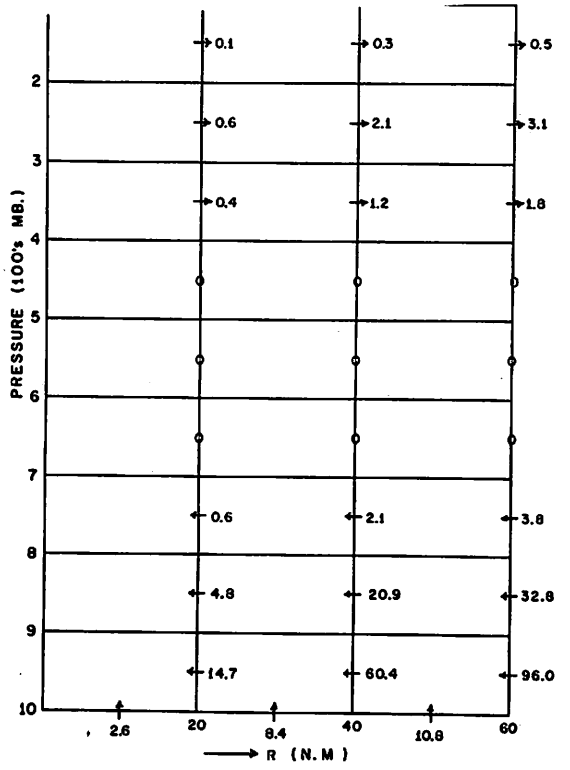

Figure 12. - Divergence of moisture, units 10^9 gr./sec.

Table 6. - Divergence of moisture and precipitation rates. Total rainfall during cyclone passage based on movement of 10 kt.

Radial interval (n. mi.)	0-20	20-40	40-60	0-60
Div q ($x10^{-9}$ g./sec.)	21.6	69.2	58.2	149.0
Rainfall (in./day)	17.0	17.8	9.3	13.1
Total rainfall during cyclone passage (in.)	2.80	2.96	1.52	7.28

8. SUMMARY AND CONCLUSIONS

In the main the Helene calculations support the results obtained for Daisy by Malkus and Riehl, although the Helene data do not permit one to perform all the computations that were made for the Daisy flights. Of major interest is the presence of the large amount of internal friction which both sets of calculations show. If subsequent calculations made with more accurate data confirm the magnitude of the internal friction, its importance in the life cycle of the tropical cyclone may be far reaching.

The Helene computations suggest that the surface exchange coefficients for heat and moisture are somewhat larger than the corresponding exchange coefficient for momentum. This variation is in the expected sense, and presumably reflects the effect of buoyant forces on the vertical fluxes. Much of the validity of the calculations for both Daisy and Helene, however, depends to a large degree upon the proper choice of the coefficients of vertical and lateral exchange, and how these vary with elevation, wind speed, atmospheric stability, etc. Calculations such as these indicate that an important advance in our understanding of some fundamental phases of the hurricane mechanism may be made as soon as the proper values of the exchange coefficients are established. It is therefore urgent that a program to determine these coefficients in tropical cyclones be undertaken.

ACKNOWLEDGMENT

The writer expresses his appreciation to Dr. Herbert Riehl, Colorado State University (formerly of the University of Chicago), who suggested the topic for this paper and offered many helpful suggestions.

REFERENCES

1. J. A. Colón et al., "On the Structure of Hurricane Daisy," National Hurricane Research Project Report No. 48, 1961, 102 pp.
2. T. H. Ellison, "Turbulent Transport of Heat and Momentum from an Infinite Rough Plate," Journal of Fluid Mechanics, vol. 2, 1957, pp. 456-466.
3. L. A. Hughes, "On the Low Level Structure of Tropical Storms," Journal of Meteorology, vol. 9, No. 6, Dec. 1952, pp. 422-428.
4. E. S. Jordan, "An Observational Study of the Upper Wind Structure Around Tropical Storms," Journal of Meteorology, vol. 9, No. 5, Oct. 1952, pp. 340-346.
5. C. L. Jordan, "Mean Soundings for the West Indies Area," Journal of Meteorology, vol. 15, No. 1, Feb. 1958, pp. 91-97.
6. D. W. Krueger, "A Relation Between the Mass Circulation Through Hurricanes and Their Intensity," Bulletin of the American Meteorological Society, vol. 40, No. 4, Apr. 1959, pp. 182-189.
7. J. Malkus and H. Riehl, "On the Dynamics and Energy Transformations in Steady State Hurricanes," National Hurricane Research Project Report No. 31, 1959, 31 pp.
8. B. I. Miller, "The Three Dimensional Wind Structure Around a Tropical Cyclone," National Hurricane Research Project Report No. 15, 1958, 41pp.
9. H. A. Panofsky, A. K Blackadar, and G. E. McVehil, "The Diabatic Wind Profile," Quarterly Journal of the Royal Meteorological Society, vol. 86, No. 369, July 1960, pp. 390-398.
10. E. Palmén and H. Riehl, "Budget of Angular Momentum and Energy in Tropical Cyclones," Journal of Meteorology, vol. 14, No. 2, Apr. 1957, pp 150-159.
11. H. Riehl and J. Malkus, "Some Aspects of Hurricane Daisy (1958)," National Hurricane Research Project Report, No. 46, 1961.
12. H. Riehl, "On the Mechanisms of Angular Momentum Transport in Hurricanes," Journal of Meteorology, vol. 18, No. 1, Feb. 1961, pp. 113-115.
13. R. H. Simpson and H. Riehl, "Mid-Tropospheric Ventilation as a Constraint on Hurricane Development and Maintenance," Proceedings, First Technical Conference on Hurricanes, Miami Beach, Fla., 19-22 November 1958.
14. Staff, Weather Bureau Office, Miami, Fla., "The Hurricane Season of 1958," Monthly Weather Review, vol. 86, No. 12, Dec. 1958, pp. 477-485.
15. R. J. Taylor, "Similarity Theory in the Relation Between Fluxes and Gradients in the Lower Atmosphere," Quarterly Journal of the Royal Meteorological Society, vol. 86, No. 367, Jan. 1960, pp. 67-78.

USCOMM-WB-DC